Journal of Corrosion and Materials
www.corromat.com

J. Corros. Mater. (2022) 1(2), 74–92.

Adsorption - Driven Interfacial Consolidation of Equisetum arvense Extract on Carbon Steel in Hydrochloric Acid

Michio Aoyama[1,*], Abdullah Al-Qahtani[2]

[1] *Institute of Environmental Radioactivity, Fukushima University, Tsukuba, Japan*
[2] *Mechanical Engineering Department, King Fahd University of Petroleum and Minerals, Saudi Arabia.*
*Corresponding author: r706@ipc.fukushima-u.ac.jp
[2]abdullahalqahtani264@gmail.com

(Received: 25 July 2022. Received in revised form: 18 September 2022. Accepted: 29 October 2022. Published online: 30 December 2022.)

Abstract

Hydrochloric-acid treatment is used to clean up the mineral deposits on steel-based desalination and water purification systems. However, the same medium promotes carbon steel dissolution by the proton reduction mechanism, chloride-enhanced corrosion and stripping of thin oxide layer. This work is aimed at finding out whether *Equisetum arvense* aerial part (EAAP) extract stabilizes the organic-metal interface under the conditions of 2 M HCl solution and what experimental criteria distinguish a transition from partial to significant inhibition. For that purpose the following parameters were examined: chemical composition of the EAAP, gravimetric weight loss, potentiodynamic polarization measurements, electrochemical impedance spectroscopy, temperature effect, adsorption properties, quantum-chemical descriptors, molecular dynamics adsorption energy and morphological structure of the surface. It is shown that HPLC analysis revealed twelve oxygenated phytochemicals, such as caftaric acid, kaempferol glycosides, quercetin-3,7-di-*O*-glucoside, isoquercetin, astragalin, and cichoric acid. IR bands at 3260/cm, 2169/cm, 1606/cm, 1518/cm, 1440/cm correspond to hydroxyl, aliphatic, carbonyl and deformation vibrations characteristic of adsorption active groups. With a concentration of 300 mg/L at 298 K, EAAP inhibits the corrosion process by reducing the corrosion rate from 12.23 ± 0.33 µg/(cm^2 h) to 0.58 ± 0.02 µg/(cm^2 h), lowers the corrosion current density from 511.5 µA/cm^2 to 13.2 µA/cm^2, and increases the charge-transfer resistance from 35.7 Ω cm^2 to 1054.9 Ω cm^2. This major change occurs within the range of 50 mg/L and 100 mg/L, with all three corrosion parameters changing at the same time. According to the activation energy, Langmuir, DFT, MD, and SEM data, the inhibition of the EAAP corrosion is caused by a mixed layer of physical and chemical adsorption where glycosylated flavonoids provide extensive surface contact while phenolic acids help occupy local sites. The combined results indicate that high inhibition cannot be described only by dosage; it is the result of interfacial consolidation where molecular identity, surface coverage, and charge-transfer limitation interact with each other.

Keywords: carbon steel; equisetum arvense; hydrochloric acid; green corrosion inhibitor; electrochemical impedance spectroscopy; adsorption; molecular dynamics.

1. Introduction

Carbon steel is still a key material for desalination equipment, water treatment units, cleaning circuits, pipelines, storage tanks, and heat-transfer auxiliary equipment because of the optimal balance of strength, weldability, machinability, availability, and low price. However, in many aqueous media, carbon steel is thermodynamically unstable and even more unstable in acid cleaning agents. Hydrochloric acid is efficient for dissolving carbonate and mixed mineral scales. However, it makes the steel substrate exposed to high proton concentration and chloride ion concentration. This means that the cleaning process that ensures the removal of fouling deposits and restoration of heat and mass transfer can provoke the fast metal loss and decreased service life of equipment at the same time. Scaling experiments in desalination explain the necessity of cleaning and fouling control in water treatment infrastructure [1]. Scale inhibitor work explains the importance of chemical conditioning of the process [2]. Corrosion engineering publications explain why carbon steel is still vulnerable in corrosive media [3]. Desalination review articles confirm the importance of material protection in water treatment systems [4].

The main steps of the electrochemical process in the case of hydrochloric acid are the anodic dissolution of iron and the cathodic hydrogen evolution. At anode regions, the iron atoms are dissolved as ferrous species. At cathode regions, the protons are reduced, and hydrogen gas is evolved. Chloride ions accelerate this process by adsorbing on the metal surface and destabilizing oxide layer, providing electrical conductivity, and facilitating the transportation of the soluble species. There are various factors influencing the rate of the process such as the concentration of the acid, temperature, flow velocity, exposition time, oxygen content, metallurgy, surface roughness, and availability of adsorption sites. Thus, acid cleaning is the chemically useful but metallurgically hazardous process. Corrosion inhibitors are used in order to interfere at the metal–solution interface, where a small quantity of the organic material can occupy the active sites, reorganize the electric double layer, and increase the energy barrier for the charge transfer. Inhibition theory explains the protection through

adsorption and blocking processes [5]. Studies of acidizing inhibitors also highlight this process in hydrochloric-acid media [6]. Modern reviews stress the importance of the interfacial interaction rather than concentration of green inhibitors [7].

Organic corrosion inhibitors usually act due to the combination of the electrostatic forces, donor–acceptor interactions, hydrogen bonding, hydrophobic repulsion, and steric blocking. Various types of molecules with the presence of oxygen, nitrogen, sulfur, phosphorus, aromatic rings, multiple bonds, and conjugated structure tend to adsorb more intensively due to the capability to provide electron density to the vacant metal orbitals or interact with the charged interfacial layer. Earlier works on the synthetic inhibitors in the acidic media revealed that the planar structure, heteroatoms, protonation degree, and adsorption geometry are critical for the inhibition process. Benzimidazole-type inhibitors illustrate the role of the heteroatom-containing organic molecules in the corrosion inhibition in acidic media [8]. Hydrazide derivatives illustrate the effect of the functionality on the steel protection in acidic solutions [9]. Computational adsorption models describe the interaction between the inhibitors and metal surfaces [10]. All the features mentioned above also relate to the plant extracts. However, there are some complications because the extract is not a single molecule but the multicomponent mixture with various phytochemicals like phenolic acids, flavonoids, glycosides, tannins, terpenoids, sugars, alkaloids, and organic acids, which can compete for adsorption sites.

The modern studies on the green inhibitors have moved away from the simple screening of the candidates towards the validation of the mechanism of protection using multitechnique approach. Review papers and recent corrosion studies stress that the botanical inhibitor cannot be considered as efficient just because of being natural or renewable. There must be the proof of the metal-loss reduction, electrochemical corrosion kinetics inhibition, impedance data on film formation, identification of functional groups, adsorption modelling, and surface confirmation. Reviews of the recent green inhibitors highlight the importance of the chemical and electrochemical validation [11]. The plant-extract corrosion studies also stress the importance of extract composition and reproducibility [12]. The assessment of the natural inhibitors suggests that the combination of experimental and computational methods can be used for evaluation [13]. The fresh plant-extract studies on mild steel in acidic media illustrate this trend. Leaves of *Falcaria vulgaris* were tested electrochemically and by surface methods [14]. The marjoram-based extracts illustrate another example of the multitechnique study of the botanically derived inhibitor [15]. *Viola* extract was tested for acid corrosion protection [16]. Essential oil of *Cuminum cyminum* illustrates the importance of the volatile phytochemical mixtures [17]. Leaves of *Pistia stratiotes* also confirm that the plant extracts require the chemical, electrochemical, and surface confirmation [18]. All these works confirm that adsorption, compactness of the film, and molecular structure must be considered together.

Equisetum arvense, also called as field horsetail, is of great importance for the present discussion because of the high variety of the oxygen-containing phytochemicals found in the aerial parts of this plant. Genus *Equisetum* is known for the presence of phenolic compounds, flavonoid derivatives, silica-related plant structure, and the polar compounds which can participate in surface interactions [19]. In the corrosion science, earlier work has shown that the *E. arvense* extract has the inhibition effect on the A36 steel in sulfuric acid, which means that this plant family possesses anticorrosion properties in one corrosive medium [20]. The hydrochloric-acid system is different from the sulfuric-acid system because of the chloride ions, acid strength, flow conditions, and the cleaning environment. Therefore, the hydrochloric-acid case requires the direct correlation between the plant chemistry and carbon steel behavior in the 2 M HCl.

The other reason for the careful approach is the nature of the inhibition process during the acid cleaning. The additive must be enough adsorptive for protecting the steel, enough soluble or dispersible for functioning in the acid cleaning bath, and compatible with the scale dissolution for not neutralizing the cleaning action. The substance which only reduces acidity can seem to be protective in the short coupon test, but it will be inefficient for the cleaning service because of the decreasing of the ability of the acid to dissolve the deposits. On the contrary, substance which adsorbs too weakly will not survive in flowing acid or thermal disturbances. The most efficient inhibitor will be the substance which acts at the metal-solution interface and forms the protective layer which delays the metal dissolution and leaves the bulk acid chemically active. This issue is especially relevant to the desalination and water treatment equipment because of the economical benefit of cleaning which consists in the recovery of heat and hydraulic performance without metal loss and creation of the rough surface, which can cause fouling.

The sustainability advantage of the botanical inhibitor requires the nuance. Extracts are usually suggested as the environmentally acceptable alternatives to the conventional synthetic inhibitors. However, this argument is plausible only when the performance of the extract is correlated with the identified chemistry, reasonable dosage, reproducible preparation, and mechanistic evidence. The high concentration of the poorly characterized extract is not necessarily more practical than the low concentration of well-characterized synthetic inhibitor. The recent review paper stresses that the green inhibitor study must involve not only efficiency but also the extract composition, corrosive medium, exposure conditions, adsorption behavior, and surface state [11]. Related plant-extract studies also support the combination of performance and chemical information [12]. The EAAP extract offers this kind of evaluation because of the chemical, electrochemical, thermal,

computational, and surface information.

The research question which is raised in the present study is whether EAAP extract forms the coherent inhibition state in the 2 M HCl through the interfacial consolidation and what combination of measurements proves this process most efficiently. This question is more precise than the question about the inhibition of the corrosion. It requires the explanation of the correlation between the HPLC-identified molecules and FTIR-active groups and reduced corrosion rate, current density, charge-transfer resistance, activation parameters, adsorption behavior, molecular orientation, and surface morphology. Moreover, the concentration interval in which the interfacial state changes most significantly is also of interest. The analysis shows that the decisive change takes place not at the highest concentration, but in the transition from the partial coverage at 50 mg/L to the significant protection at 100 mg/L. Then, this change evolves moderately between 100 mg/L and 300 mg/L, which means that the active-site occupation is the limiting factor after the formation of the phytochemical layer.

The chemical characterization is conducted to determine the functional composition of the extract prior to the corrosion inhibition study. Gravimetric analysis establishes whether the inhibitor leads to a reduction of material loss during the exposure. Polarization curves evaluate whether anodic and cathodic reactions are inhibited. Impedance measurements determine whether a more resistive and less capacitive interfacial layer is formed. Temperature studies explore the stability of this layer upon heating of the acid medium. The mechanisms of the adsorption process and its results can be explored by adsorption, DFT, molecular dynamics, and SEM techniques. The importance of this sequence is that no single experiment bears full responsibility for the mechanism proof.

2. Materials, Exposure Conditions, and Calculations

The experimental system is a corrosion inhibitor consisting of EAAP extract for carbon steel in acid-cleaning environment similar to multi-stage-flash desalination equipment [21]. Carbon steel was obtained from an Egyptian thermal water treatment plant and had 0.23 wt.% C, 0.035 wt.% P, 0.007 wt.% Si, 0.34 wt.% Mn and iron as a remainder in its composition. Corrosive medium was 2.0 M HCl made up from analytical-grade hydrochloric acid. It is a reasonable choice for acid cleaning medium because both proton and chloride activities are high enough to stimulate uniform and pitting corrosion of steel. Usage of plant extract as an inhibitor in such medium is a challenging test of the interfacial protection rather than simple screen.

The inhibitor was extracted from 10 g of *E. arvense* aerial parts powder in 100 mL of solvent containing 8% ethyl acetate, 22% distilled water and 70% ethanol. The mixture was stirred and heated at 348 K for 5 h, was cooled for 72 h, vacuum-filtered and evaporated at 313 K till removal of solvents. This method is chemically justified due to water–ethanol mixture that allows to extract polar compounds such as phenols and glycosides and ethyl acetate that enables access to moderately polar aromatic compounds. Concentrations of 25 mg/L, 50 mg/L, 100 mg/L, 200 mg/L and 300 mg/L were tested in acid. Such range of concentrations is wide enough to separate the cases of weak adsorption and near saturation, and to check whether the behavior is smooth or there is a sharp change.

Characterization of chemical composition of the extract is carried out by high-performance liquid chromatography and Fourier-transform infrared spectroscopy. HPLC was used to establish major components and their retention times, whereas FTIR was used to characterize functional groups of the extract by measuring absorption in 4000–400/cm range with KBr plates. These two methods give complementary data. HPLC gives molecular identity, and FTIR gives information about the functional bonds. Both are needed in case of multicomponent extract because the corrosion inhibition cannot be established by means of one peak or one functional group.

The carbon steel coupons used in mass-loss test were sized $1.0 \times 1.5 \times 0.05$ cm and were polished with emery papers up to 800–2800 grade. Immersion time was 4 h. Flow velocity of the solution was kept constant at 2.0 m/s under aerated conditions that is important since in the plant equipment acid cleaning medium is not stagnant but circulating. Evaluation of samples was performed according to ASTM G1-03 standard [22]. The corrosion rate was calculated as

$$CR = \frac{W}{At}, \tag{1}$$

where W is mass loss, A is exposed surface area, and t is exposure time. The inhibition efficiency from mass loss was calculated as

$$\eta_W(\%) = \frac{CR_0 - CR}{CR_0} \times 100, \tag{2}$$

where CR_0 is the corrosion rate in uninhibited acid. These expressions are deliberately kept simple, but their practical usefulness cannot be overestimated: they determine if the inhibition of the material loss due to inhibitor adsorption is observed under given exposure conditions.

Electrochemical measurements were performed using a three-electrode cell, where the working electrode was made of carbon steel, the reference one was a saturated calomel electrode and the counter one was a platinum wire. The active

surface of the working electrode had the area of 0.564 cm^2. The open-circuit potential equilibration time was 60 min. Potentiodynamic polarization curves were registered with the scan rate of 1.25 mV/s. The inhibition efficiency of the extract due to corrosion current density change was defined as

$$\eta_j(\%) = \frac{j_{\mathrm{corr},0} - j_{\mathrm{corr}}}{j_{\mathrm{corr},0}} \times 100. \tag{3}$$

The given value is more than just the percent. It represents the suppression power of the extract on the electrochemical reaction rate at the corrosion potential and thus allows to differentiate between the cases when the surface was blocked and when it was only cleaned after exposure.

For the EIS experiment, the frequency range was set from 100 kHz to 0.01 Hz with an amplitude of 20 mV applied at open-circuit potential. The EIS spectra were fitted by the circuit consisting of solution resistance, charge transfer resistance and constant phase element. Application of a constant phase element is justified by the fact that corroding surfaces of steel in acidic chloride solutions hardly ever act as ideal capacitors owing to roughness, heterogeneous adsorption, porosity of corrosion products, and uneven distribution on the surface [23]. Inhibition efficiency based on impedance measurements was determined by formula

$$\eta_R(\%) = \frac{R_{ct} - R_{ct,0}}{R_{ct}} \times 100. \tag{4}$$

Consistency among Eqns. (2), (3), and (4) is crucial since these three equations examine the state of inhibition from different perspectives. Mass loss represents the cumulative effect of damage over time, while polarization and impedance examine the kinetic properties of corrosion and the resistance of the interface, respectively.

Mass loss versus temperature was analyzed between 298 K and 328 K in blank acid and acid with 300 mg/L EAAP. The apparent activation energy for these reactions was calculated using the Arrhenius equation

$$CR = A \exp\left(-\frac{E_a}{RT}\right), \tag{5}$$

and activation enthalpy and entropy were obtained from the transition-state relation

$$CR = \frac{RT}{Nh} \exp\left(\frac{\Delta S^*}{R}\right) \exp\left(-\frac{\Delta H^*}{RT}\right). \tag{6}$$

Such values were considered to be the indices of the effect of the inhibitor on the dissolution mechanism. The increase of the value of E_a or ΔH^* in the inhibited solution means that the adsorbed layer increases the activation energy of the corrosion reaction, whereas a negative value of ΔS^* means an increased order of the activated complex related to organic compounds.

Adsorption was determined by the Langmuir equation

$$\frac{C_{\mathrm{inh}}}{\theta} = \frac{1}{K_{\mathrm{ads}}} + C_{\mathrm{inh}}, \tag{7}$$

where C_{inh} is inhibitor concentration, θ is surface coverage, and K_{ads} is the adsorption equilibrium constant. The Langmuir equation is still used as an approximation to apparent site occupation, but one should not interpret this equation as evidence that a homogeneous chemical monolayer is formed. EAAP consists of a set of molecules differing from each other by size, polarity, protonation and adsorption properties. The original Langmuir theory gives the classical expression for the relationship between the surface coverage and adsorption equilibrium [24]. From the point of view of corrosion inhibition practice, the more correct approach would be the statement that the total surface coverage is described by the Langmuir behavior despite the heterogeneity of the molecular film [25].

Four major components were examined computationally: caftaric acid, kaempferol-3,7-di-*O*-glucoside, kaempferol-3-*O*-rutinoside, and isoquercetin. The quantum descriptors consisted of the following parameters: HOMO energy, LUMO energy, HOMO-LUMO gap, ionization potential, electron affinity, dipole moment, electronegativity, hardness, and electron transfer fraction. Adsorption in molecular dynamics on Fe(110) was studied by

$$E_{\mathrm{ads}} = E_{\mathrm{total}} - (E_{\mathrm{surf+water}} + E_{\mathrm{inh+water}}) + E_{\mathrm{water}}. \tag{8}$$

The negative adsorption energy signifies a favorable interaction with the surface. The benefit of such an approach is that it allows correlating the efficiency of the inhibitor with its surface interaction geometry rather than bulk concentration. Such an approach is becoming increasingly common in the quantum-chemical study of plant extract inhibitors since the most effective inhibitors are often those with electron-rich groups and proper geometry allowing extensive interaction with the surface. Electronic description of inhibition is discussed in quantum-chemical studies of natural inhibitors [26]. Relationship between adsorption geometry and surface protection is addressed in molecular dynamics studies [27]. An example of computational and experimental studies of a plant extract inhibitor is provided by the recent work on marjoram extract [15].

The consistency between three independent efficiencies of inhibition is crucial for understanding of the process. While the gravimetric efficiency is important due to accounting the cumulative steel loss, it cannot distinguish between anodic and cathodic processes. The polarization efficiency depends on accurate Tafel extrapolation and stability of the corrosion potential during electrochemical scan. The impedance efficiency is influenced by interfacial resistance and the film density; it also depends on the suitability of the equivalent circuit used. The presence of the same trend in three different efficiencies independently provides much more convincing evidence compared to any individual percent. Therefore, the discussion focuses on the interval from 50 mg/L to 100 mg/L, when all three efficiencies sharply change.

Second, the inhibitor film is considered chemically heterogeneous. Langmuir model can be used for estimating the average surface coverage of inhibitor, but EAAP contains acids, flavonoid glycosides, and other molecules with diverse molecular areas and interaction possibilities. One-site adsorption equation describes the average relationship between concentration and coverage; it does not require that every molecule interacts identically with the surface. This distinction prevents the overinterpretation of the adsorption plot. It also explains why the results of the computational study of the selected molecules should be interpreted as properties of the main components of the inhibitor rather than as the complete list of the inhibitor molecules. The strongest mechanistic conclusion from this study is not that one molecule alone controls the inhibition process; the conclusion is that certain molecules form a heterogeneous surface film that provides the high resistance to charge transfer and reduced water and chloride penetration.

3. Results and Discussion

3.1 Phytochemical identity and functional basis of adsorption

HPLC analysis revealed twelve principal components in the EAAP extract, as shown in Table 1. Unlike many other inhibitor systems, EAAP extract contains multiple compounds, including both acids and glycosylated flavonoids. This chemical diversity is critical for the mechanism of inhibition because the surface of carbon steel in 2 M HCl solution is chemically heterogeneous. Different iron sites, chloride-modified regions, regions with incipient corrosion products, and hydrogen evolution sites do not offer similar adsorption environment. In the case of a mixture of molecules, this heterogeneity can allow better protection compared to single inhibitor, since small molecules fill available sites, whereas large flavonoids can interact with broader surface areas.

Table 1: EAAP compounds.

Peak	t_R (min)	Formula	Compound
1	8.7	$C_{13}H_{12}O_9$	Caftaric acid
2	12.2	$C_{33}H_{40}O_{21}$	Kaempferol 3-sophoroside-7-glucoside
3	15.7	$C_{27}H_{30}O_{17}$	Quercetin-3,7-di-*O*-glucoside
4	17.1	$C_{13}H_{12}O_8$	Caffeoyl-malic acid
5	21.2	$C_{27}H_{30}O_{16}$	Kaempferol-3,7-di-*O*-glucoside
6	22.6	$C_{27}H_{30}O_{15}$	Kaempferol-3-*O*-rutinoside
7	25.8	$C_9H_8O_3$	Coumaric acid
8	26.9	$C_{10}H_{10}O_4$	Methyl caffeate
9	28.7	$C_{21}H_{20}O_{12}$	Isoquercetin
10	29.4	$C_{21}H_{20}O_{10}$	Apigenin-*O*-glucoside
11	30.8	$C_{21}H_{20}O_{11}$	Astragalin
12	32.5	$C_{22}H_{18}O_{12}$	Cichoric acid

The above-mentioned compound distribution (Table 1) offers a solid chemical rationale for adsorption. The compounds such as caftaric acid, caffeoyl-malic acid, coumaric acid, methyl caffeate, and cichoric acid contribute carboxyl, hydroxyl, carbonyl and aromatic groups. Kaempferol derivatives, quercetin-3,7-di-O-glucoside, isoquercetin, apigenin-O-glucoside, astragalin are also included and they provide a big aromatic surface area and several oxygen centres. Thus, the extract has groups capable to undergo protonation reaction under acidic conditions, electrostatic interaction by means of chlorine-mediated surface charges, hydrogen bonding in the interfacial layer, as well as electron donation to iron centres. Analogous functions were attributed to oxygen-containing plant extracts from liquorice [28]. Extract from gooseberry shell is yet another example of the phytochemicals adsorption in acidic solutions [29]. Another similar extract from *Sida acuta* was used to explain the protection of metals from corrosion in the presence of plant extract covering the metal surface by organic molecules [30]. Yet another example is provided by bamboo leaf extract to show the contribution of oxygenated plant components to steel protection [31]. The extract from marigold flowers also highlights the importance of phenolic and

aromatic components [32]. The extract from ginkgo leaves also emphasizes the fact that oxygen-bearing plants can work as inhibitors to corrosion [33].

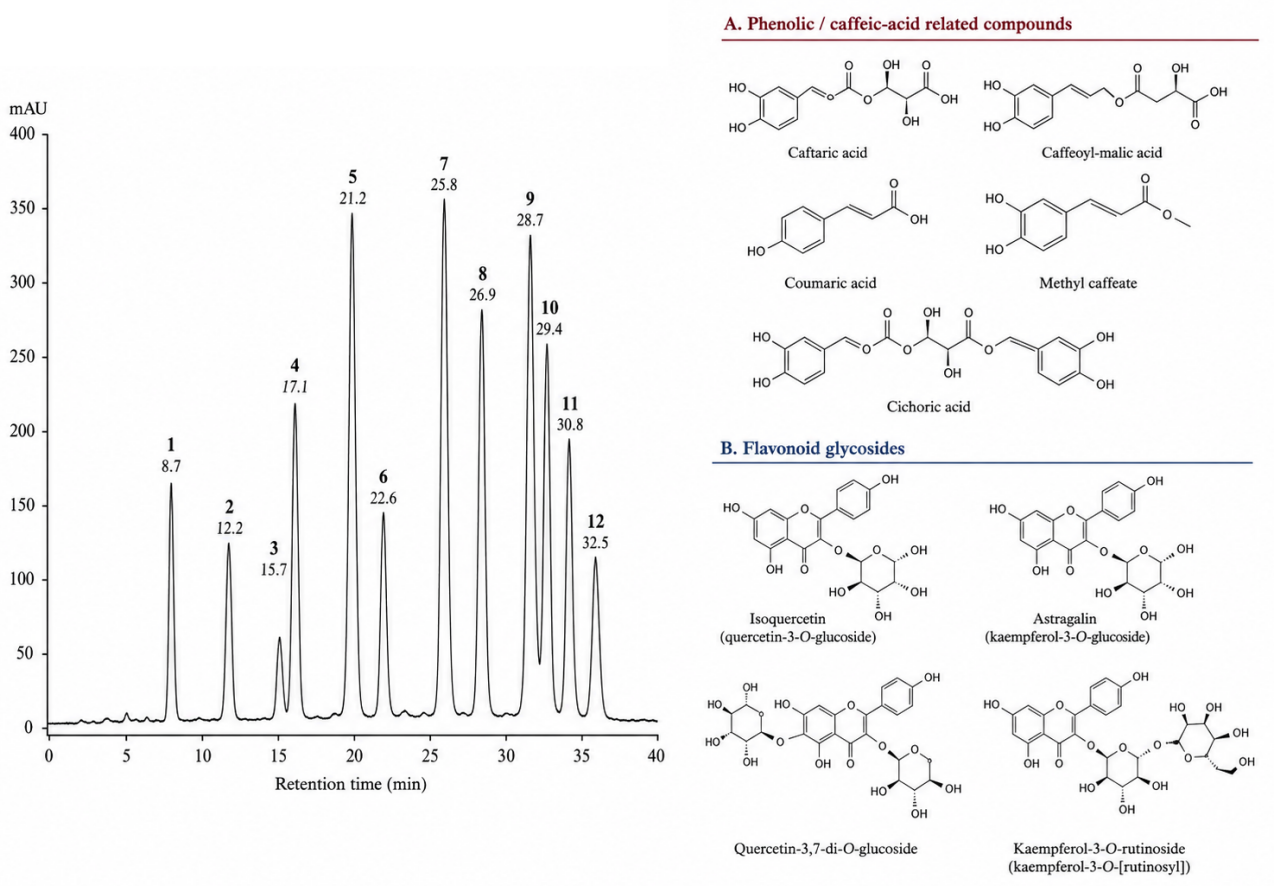

Figure 1: EAAP chemistry.

This figure 1 is also instructive regarding the mechanism behind the fact that the extract does not have a linear dependence between concentration and effectiveness of adsorption. The retention time indicates that there are both polar phenolic acids that elute relatively early and the later flavonoids. Their simultaneous presence creates conditions under which two kinds of adsorption interactions can proceed concurrently. Small acids can access the nearby active adsorption sites, while the larger glycosides can sit parallel to the iron surface. Therefore, the expected cooperative effect should start after some number of molecules are available for both types of adsorption sites.

The FTIR assignment explains the nature of these adsorption sites. The band near 3260/cm corresponds to O–H stretch, meaning that the extract contains carboxylic and phenolic groups. The band near 2169/cm corresponds to aliphatic C–H. The carbonyl functionality is reflected in the 1606/cm band. The C=O stretching and C–H deformation correspond to the bands near 1518/cm and 1440/cm. Apart from being mere assignments, this information is important in the context of corrosion inhibition of steel. Hydroxyl and carbonyl groups are major binding sites for the inhibitors, aromatic rings and conjugation allow planar adsorption and hydrophobic shielding, and glycosidic oxygens increase local polarity.

The FTIR assignment clarifies why this inhibitor behaves in a particular way when coming into contact with strongly acidic solution. Phenolic and carboxylic groups can become partially protonated, increasing their electrostatic interaction while still maintaining the oxygen atoms needed for polar adsorption. Hence, the inhibitor molecules can possess both solution-phase mobility and adsorption properties. Another aspect of aromatic rings is that they serve a different purpose by not just anchoring the molecule but providing shielding once the molecule adsorbs. Studies of benzimidazole-based inhibitors illustrate the role of heteroatoms and aromatic rings in the process of acid corrosion protection [8]. The computational analysis of adsorption elucidates the importance of polar adsorption sites and geometric properties of the adsorption interface [10]. Review articles on modern inhibitors highlight the common properties of effective inhibitors: polar anchoring sites and hydrophobic shielding [7].

This chemical consideration leads to one conclusion regarding the use of this inhibitor in practice. EAAP cannot precipitate an insoluble inhibitor from the bulk acid in order to form the protective layer. The extracted molecules are mostly the oxygen-containing organic molecules that will remain dispersed in the acid and move toward the metal boundary. The described property is more appropriate for acid cleaning than bulk precipitation because the precipitated layer will block the

movement of the liquid. In contrast, the inferred mode of protective action involves adsorption at the steel dissolution sites.

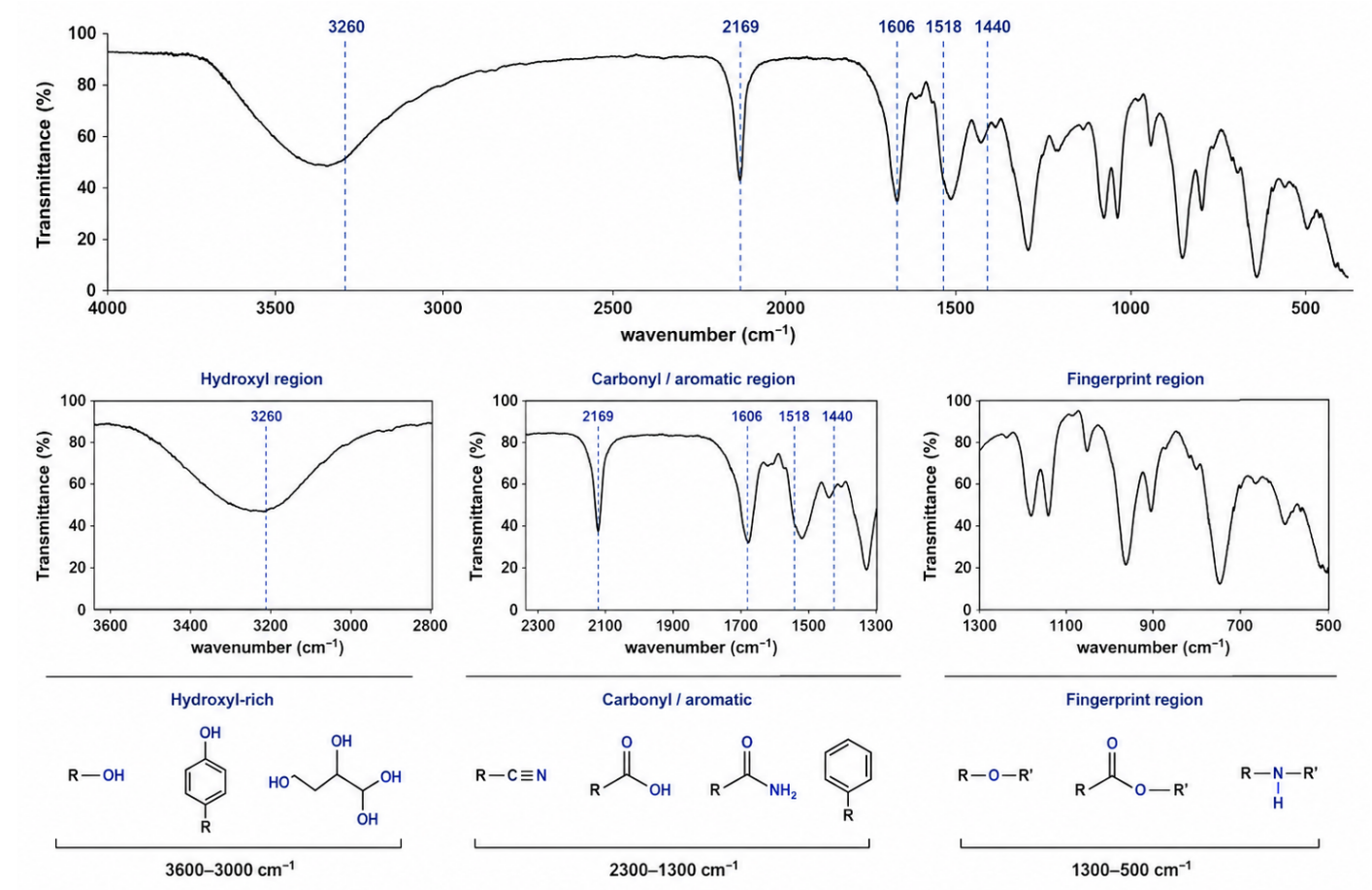

Figure 2: FTIR groups.

The relationship between the spectral profile (Figure 2) and the electrochemical behavior of the sample is thus established. Should the extract consist of predominantly nonpolar substances without any donor atoms, an extreme reduction in capacitance and an extreme rise in the charge transfer resistance are unlikely to be expected. Instead, the FTIR analysis suggests that the extract contains the functional groups necessary to displace the water-chloride containing surface layers. The functional group information opens the door for mechanism development which is then corroborated by the mass loss, polarization, and impedance.

3.2 Mass loss behavior and the effective protection range

The mass loss data (Table 2) provide the evidence that EAAP inhibits practical metal corrosion in 2 M HCl at 298 K. The blank corrosion rate is measured at 12.23±0.33 µg/(cm^2 h). When 50 mg/L, the rate drops even more to 6.38±0.24 µg/(cm^2 h), which corresponds to an efficiency of 47.8%. Both concentrations provide some kind of inhibition but the surfaces are still accessible for electrochemistry.

Table 2: Mass-loss response.

EAAP (mg L^{-1})	CR (μg cm^{-2} h^{-1})	η_W (%)	Rate reduction
Blank	12.23 ± 0.33	–	1.00
25	9.24 ± 0.42	24.4	1.32
50	6.38 ± 0.24	47.8	1.92
100	1.01 ± 0.04	91.7	12.11
200	0.62 ± 0.02	94.9	19.73
300	0.58 ± 0.02	95.2	21.09

The critical transition for mass loss happens within the range of 50 mg/L to 100 mg/L. Within this range, the corrosion rate falls from 6.38 µg/(cm^2 h) to 1.01 µg/(cm^2 h), while inhibition increases from 47.8% to 91.7%. Reduction in the corrosion rate compared to the rate of blank acid ranges from 1.92-fold to 12.11-fold.

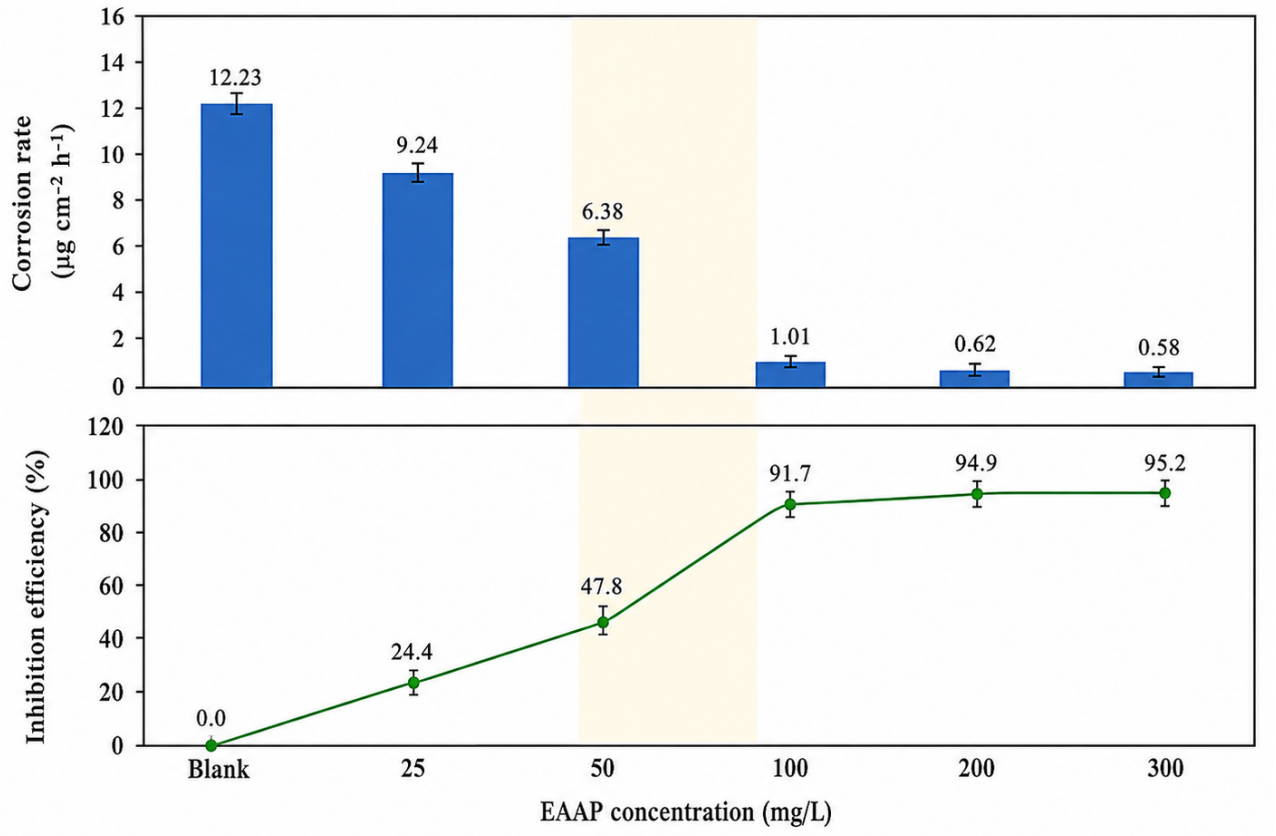

Figure 3: Mass-loss trend.

This is too high to be explained by mere dilution of reactive species or just scattered results. It shows that the steel surface goes through a coverage regime in which the extract switches from being partially covering to covering the entire surface. The improvement achieved by increasing the extract concentration from 100 mg/L to 300 mg/L is comparatively small, which suggests that most of the active sites are already occupied at 100 mg/L concentration level.

The concentration dependence in Fig. 3 also makes the same statement graphically. The slope of the curve of the corrosion rate is very large in the middle concentration range and almost zero in the high concentration range. This dependence corresponds to adsorption controlled inhibition, because when all active surface sites get occupied, additional increase of extract leads to smaller and smaller effects. There are also important practical implications. Selection of the inhibitor for acid cleaning cannot be done on the basis of the maximum obtained efficiency. The practical concentration of the inhibitor is needed which provides the sufficient protection of the interface without extra amount of the organic additive. The mass loss values reveal 100 mg/L as the first concentration providing strong protection, while 300 mg/L as the one corresponding to the maximum obtained efficiency.

The small values of the standard deviations of the high-inhibition mass loss values are also meaningful. For 200 mg/L and 300 mg/L the corrosion rates are 0.62 ± 0.02 and 0.58 ± 0.02 μg/(cm^2 h), respectively. The difference between them is very small and both values are far from the blank corrosion rate. This fact supports the idea that the high concentration range corresponds to the stable state of protection and does not continue the low concentration tendency. The practical implication is that 300 mg/L is the best value of the concentration, while 200 mg/L already provides the gravimetric inhibition regime.

The gravimetric measurements are very important due to the fact that the exposure was performed in the regime of 2.0 m/s solution velocity. The flow can wash off weakly adsorbed species, increase the transport of corrosive ions and decrease the residence time of the molecules near the metal surface. The strong mass loss inhibition in the moving acid solution implies that the EAAP layer is not restricted to weak adsorption and transient process. The film should be either rapidly reformed or have sufficient strength to resist hydrodynamic disturbances during the four-hour exposure. This point adds significance to the results obtained for the evaluation of the ability of the inhibitor to clean the circuits, where the stationary immersion can underestimate the challenge for the inhibitor.

The inhibition degree of the metal losses by EAAP is impressive compared with other green inhibitors in the acidic environments. Plant extracts usually show their high efficiency at high concentrations or under the acid conditions less severe than in this experiment. EAAP provides 95.2% gravimetric inhibition at 300 ppm in 2 M HCl, the environment being more aggressive than most of 1 M HCl. So the result is not just the illustration of the fact that the plant extract can inhibit the corrosion, but the proof that the oxygen-rich aerial-part extract can provide significant inhibition in industrially relevant

conditions of cleaning with a strong acid.

3.3 Polarization evidence for mixed electrochemical inhibition

From the polarization results in Table 3, it can be seen that EAAP strongly reduces corrosion current density and the corrosion potential is shifted to the positive direction. In the absence of any inhibitor, E_{corr} is −486 mV versus SCE and j_{corr} is 511.5 µA/cm^2. In the presence of 25 mg/L EAAP, j_{corr} becomes 329.4 µA/cm^2, showing 35.6% inhibition. In the presence of 50 mg/L of the inhibitor, it is 116.1 µA/cm^2. At 100 mg/L concentration of the inhibitor, it becomes 34.7 µA/cm^2. At 300 mg/L concentration of the inhibitor, it becomes only 13.2 µA/cm^2. The maximum efficiency at this concentration is 97.4%.

Table 3: Polarization response.

EAAP (mg L^{-1})	E_{corr} (mV SCE)	j_{corr} (μA cm^{-2})	η_j (%)
Blank	-486	511.5	–
25	-462	329.4	35.6
50	-434	116.1	77.3
100	-420	34.7	93.2
200	-407	18.4	96.4
300	-397	13.2	97.4

Maximum potential shift due to the EAAP addition is around 89 mV. The above-mentioned value is not sufficient to categorize EAAP as a pure anodic or a pure cathodic inhibitor according to the widely accepted 85 mV criterion, but the positive shift in conjunction with simultaneous reduction of current density suggests mixed-mode inhibition where more pronounced effects take place at the anodic region of the potential scale. This kind of inhibition is typical for a protective coating which prevents the iron ions dissolution and also reduces hydrogen evolution. Pure cathodic inhibitors should primarily reduce proton reduction, and pure anodic inhibitors will prevent iron oxidation.

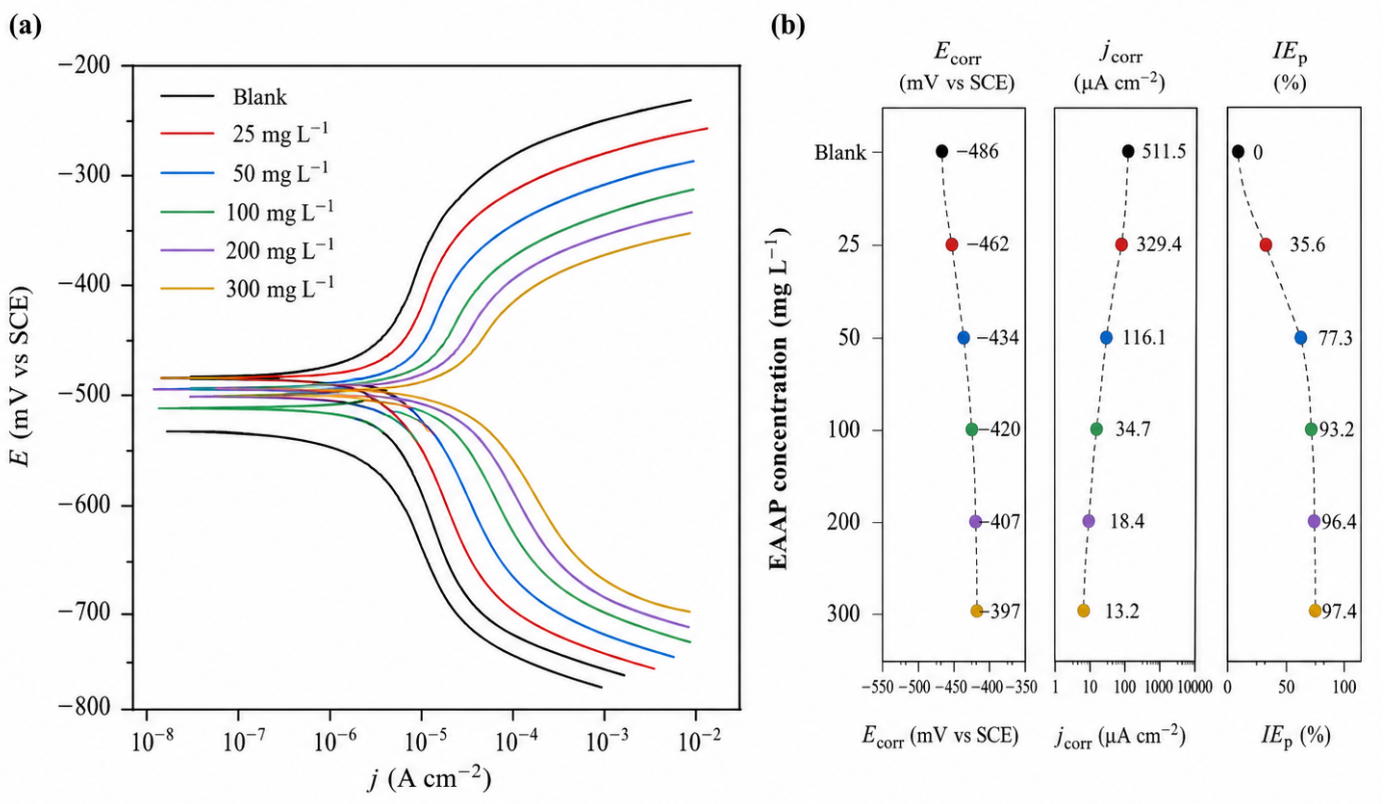

Figure 4: Polarization response.

Pattern shown in Figure 4 clearly confirms the similarity of the electrochemical transition and the transition of gravimetric protection. The reduction in current density from 116.1 µA/cm^2 at 50 mg/L to 34.7 µA/cm^2 at 100 mg/L is especially indicative since it takes place within the same concentration range where the gravimetric protection becomes effective. The consistency of gravimetric protection and polarization demonstrates that there is no risk of artifacts due to

cleaning and corrosion product removal as well as due to patchy protection of surface. It confirms that the inhibitor prevents the corrosion process during electrochemical processes.

Mixed-type of the response has certain consequences for mechanisms of action of phytochemicals. Phenolic acids and flavonoid glycosides could be adsorbed by means of oxygen centres and aromatic moieties. In acidic chloride medium, protonated molecules could form initial contact with the steel surface through electrostatic interaction while neutral or partially deprotonated molecules could participate in electron transfer via oxygen and aromatic moieties. Such type of film could not be selective for only one site of reaction. It could be formed both on anodic site of Fe dissolution and cathodic site of hydrogen evolution. An example of such a behaviour for plant-based inhibitor is olive leaf extract [34]. Another example of reduced corrosion current with partial substitution of electrochemical mechanism is marjoram extract [15]. Extract of Pistia stratiotes leaves is a rather new case when the compounds inhibit both cathodic and anodic processes [18].

3.4 Impedance response and interfacial compactness

The EIS technique gives the best proof for the fact that EAAP alters the steel/solution interface. The charge transfer resistance is increased from 35.7 Ω cm^2 in plain acid to 60.5 Ω cm^2 at 25 mg/L, 192.4 Ω cm^2 at 50 mg/L, 850.4 Ω cm^2 at 100 mg/L, 1024.8 Ω cm^2 at 200 mg/L, and 1054.9 Ω cm^2 at 300 mg/L. Impedance efficiency is reached to 96.6% at the maximum concentration. These data indicate that the inhibitor is not just retarding corrosion via changing the chemistry of the solution but is forming a film which impedes the charge transfer.

Table 4: Impedance response.

EAAP (mg L^{-1})	R_{ct} (Ω cm^2)	CPE (μF cm^{-2})	η_R (%)	$R_{ct}/R_{ct,0}$
Blank	35.7	725.4	–	1.00
25	60.5	454.7	40.9	1.69
50	192.4	276.4	81.4	5.39
100	850.4	198.3	95.7	23.82
200	1024.8	105.2	96.5	28.71
300	1054.9	89.9	96.6	29.55

There is a significant drop in constant phase element from 725.4 µF/cm^2 in blank acid to 89.9 µF/cm^2 for 300 mg/L solution. This kind of drop in constant phase element is an indicator of adsorption layer formation since organic molecules will take place of water and chloride around metal and lower dielectric constant as well as increase interfacial barrier thickness.

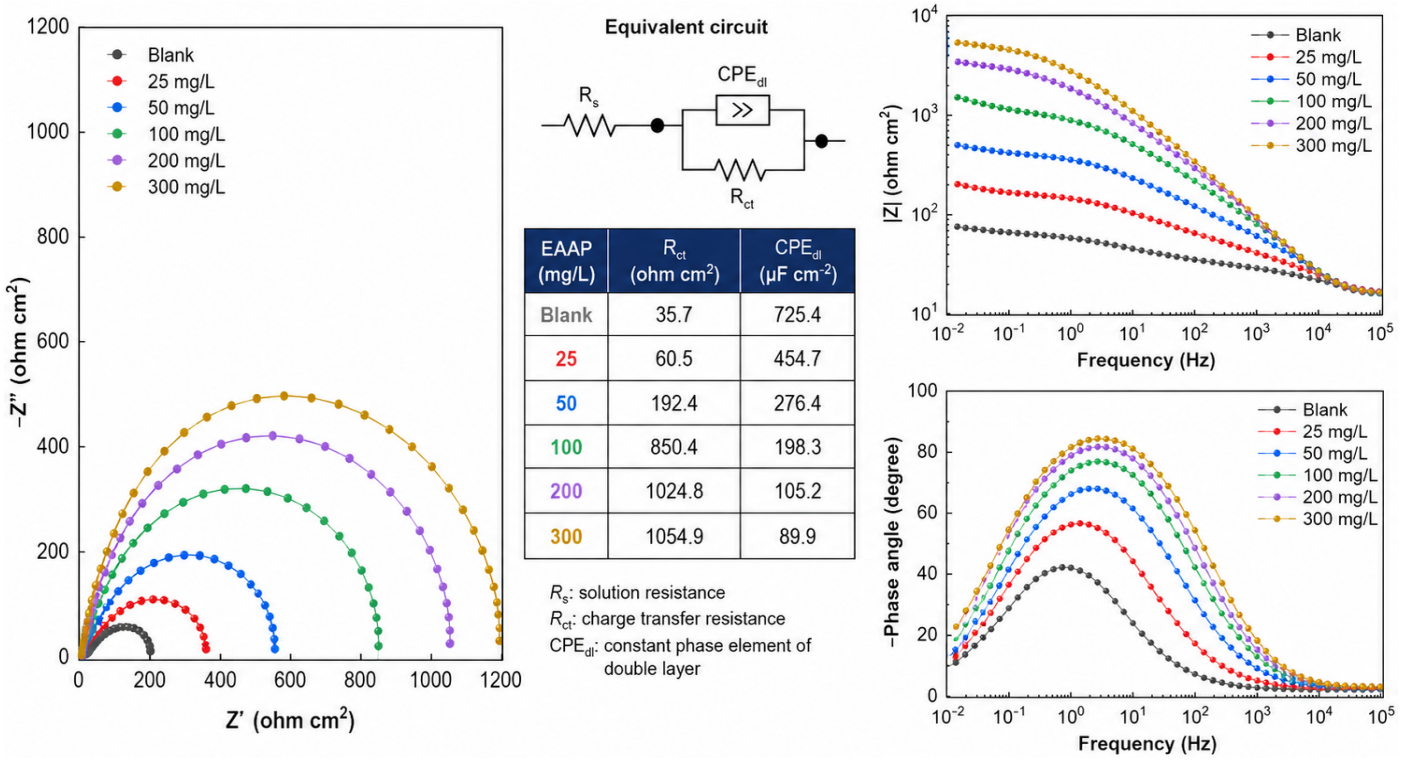

Figure 5: Impedance response.

The ratio $R_{ct}/R_{ct,0}$ gives an intuitive measure of the effect: the interface becomes 5.39 times more resistant at 50 mg/L, 23.82 times more resistant at 100 mg/L, and 29.55 times more resistant at 300 mg/L. The main resistance gain is therefore achieved by 100 mg/L, while the highest concentrations mainly refine the film.

The EIS summary shown in Figure 5 turns the claim of chemical adsorption into an electrical experiment. A thin inhibitor layer causes an increase in R_{ct} and a reduction in the capacitance. EAAP increases R_{ct} and reduces capacitance. The combined increase in R_{ct} and reduction in the CPE are consistent with the concentration range determined by the mass loss and polarization. Three different measurements confirming each other is more convincing than the single value of the efficiency. The transition point between 50 mg/L and 100 mg/L is thus an interfacial process seen via the separate experiments.

The depressed semicircle response caused by the use of a constant phase element is not a drawback of the method. It is the proper response expected for a corroding, inhibitor-coated surface of steel. Interfaces have natural microstructure and non-homogeneous chemistry. A simple ideal capacitor model would imply a perfect interface which never exists in reality. The CPE thus supports the idea of the non-uniform but efficient adsorption of the organic compound on the steel surface. The use of constant phase elements for corrosion analysis of non-ideal interfaces is common practice [23]. Impedance measurements of organic films covering rough metal surfaces also reveal depressed capacitive loops [35]. Similar phenomena were seen with complex organic inhibitors adsorbing onto the steel surface in acidic medium [36].

3.5 Thermal stability and activation energy analysis

Data measured as functions of temperature, see Table 5, confirm the increase in corrosion rate with the increase in temperature for both blank and inhibited samples. In blank 2 M HCl, the corrosion rate rises from 12.23 ± 0.33 µg/(cm^2 h) at 298 K to 21.54 ± 0.50 µg/(cm^2 h) at 328 K. With 300 mg/L EAAP, the rate rises from 0.58 ± 0.02 µg/(cm^2 h) to 2.30 ± 0.19 µg/(cm^2 h). The efficiency decreases from 95.2% to 89.3%. The decrease shows that adsorption plays a role in inhibition while thermal agitation partially reduces the effectiveness of the adsorbed layer. But the efficiency above 89% maintained even at 328 K suggests that the layer survives the heat treatment.

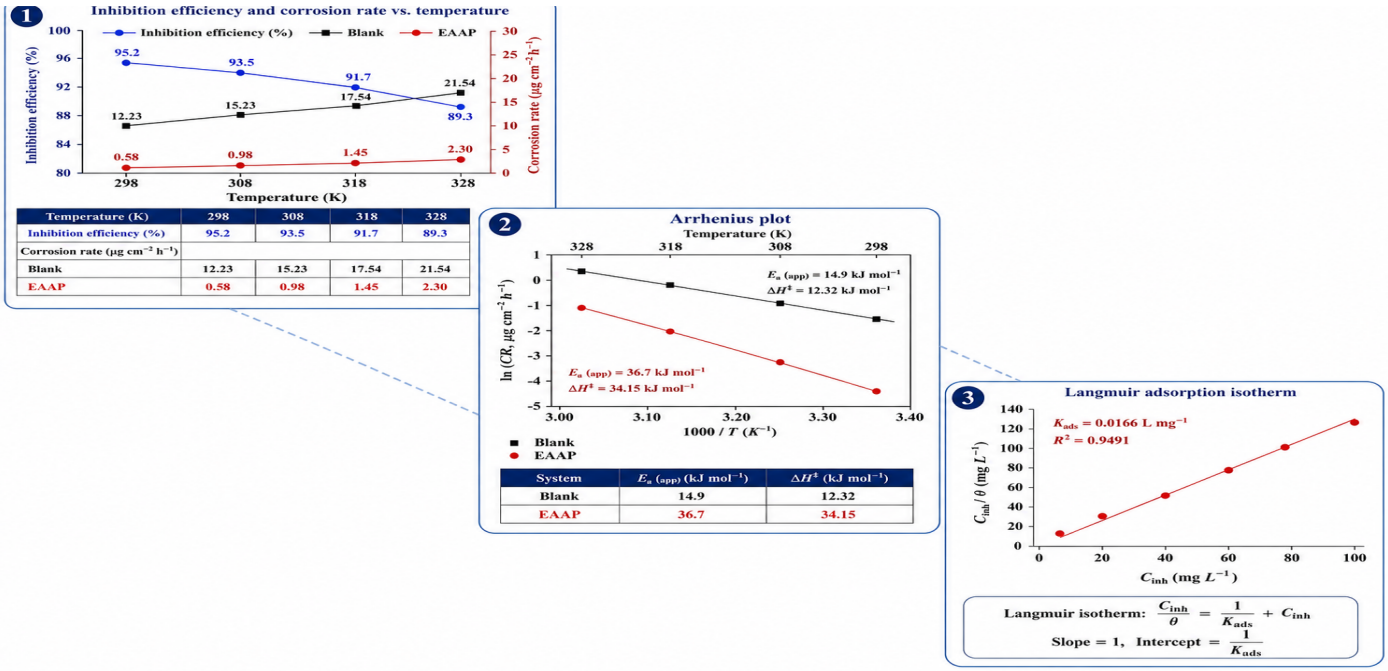

Figure 6: Heat and adsorption.

The temperature dependence in Figure 6 reveals an important aspect of mechanism. First of all, decreasing of the efficiency due to temperature increase means significant contribution of the physical adsorption due to the fragility of the electrostatic layer at higher temperatures. On the other hand, rising of the activation energy and maintaining of high efficiency show that the layer is more than just electrostatic. The most realistic mechanism in this situation is the mixed mechanism. Initial attraction may include protonated phytochemical species and modified steel, while additional stabilization includes interaction through the oxygen centers, aromatic region contact, and lateral association of the molecules from the extract.

Table 5: Temperature response.

Temperature (K)	Blank CR (μg cm^{-2} h^{-1})	EAAP CR (μg cm^{-2} h^{-1})	η_W (%)
298	12.23 ± 0.33	0.58 ± 0.02	95.2
308	15.23 ± 0.41	0.98 ± 0.12	93.5
318	17.54 ± 0.47	1.45 ± 0.15	91.7
328	21.54 ± 0.50	2.30 ± 0.19	89.3

It can be seen that the activation energy rises from 14.9 kJ/mol in blank acid to 36.7 kJ/mol in the presence of 300 mg/L EAAP. Correspondingly, activation enthalpy grows from 12.32 kJ/mol to 34.15 kJ/mol. Such growth shows that steel dissolution is becoming energetically harder due to the extract presence. The activation entropy changes from -153.2 to -224.8 J/(mol K) and reflects the increase in ordering of the activated state. This greater ordering is possible due to the adsorption of organic molecules, water structure constraining, and the decreased freedom of motion for the reagents on the metal surface.

Of course, the temperature dependence is important from practical point of view, too. Cleaning is not always carried out at the room temperature, so the inhibitors from plants have to demonstrate activity under heating in order to be technically acceptable. EAAP is not able to keep 95.2% efficiency at 328 K, but it decreases corrosion from 21.54 µg/(cm^2 h) to 2.30 µg/(cm^2 h). This is practically valuable and means that the temperature acceleration of the corrosion is compensated by the inhibitor.

3.6 Adsorption behaviour and surface-coverage logic

According to the Langmuir adsorption analysis, the correlation coefficient is equal to 0.9491, and the adsorption equilibrium constant equals 0.0166 L/mg. This means that the surface coverage is a controlling variable. This is natural for the multicomponent botanical extract. Ideal Langmuir monolayer implies identical sites without any lateral interactions and only one adsorbate. EAAP does not satisfy all these requirements: steel surface is heterogeneous, extract contains twelve identified components, and large flavonoids are able to make lateral or steric contacts with neighboring molecules. Thus, the useful implication is not the ideal behavior of the film, but its coverage-dependent efficiency.

The adsorption panel in Figure 6 explains why the mass loss, polarization, and EIS records change abruptly at the concentration of 100 mg/L. At low concentrations, many sites remain active, and the extract is able to retard, but not stop the corrosion process. When the concentration increases, the film begins to interfere with the continuity of acid and electron transport to the metal. Once the most active sites are occupied by the molecules, their addition leads to the filling of less active sites or thickening of already active protective layer. It means that the improvement is diminishing from 100 mg/L to 300 mg/L.

The meaning of K_{ads} should be interpreted carefully considering that the concentration is not measured in mol/L and the extract contains several molecules. It can be used as the apparent extract-level constant, not the molecular thermodynamic constant for one pure compound. Its low value is consistent with the physical adsorption as the main mechanism, especially taking into account the temperature dependence of the efficiency. However, physical adsorption does not imply weak activity. At the strongly acidic chloride media, rapid occupation of the charged interface by protonated or polar molecules can be very effective, especially with the support of molecular size, aromatic contact, and oxygen-rich anchoring.

The adsorption analysis is consistent with the classic corrosion inhibition principles and plant-extract experience in the literature. Langmuir-type behavior was used to interpret adsorption of the olive-leaf extract [37]. *Baphia nitida* extract is another example of the adsorption-controlled inhibition from plants [38]. The adsorption in acidic solutions was used to explain the loquat-leaf extract [39]. Marjoram extract is another confirmation of the utility of the combination of adsorption fitting and electrochemical analysis [15]. *Tectona grandis* leaf extract is another plant-extract example where electrochemical analysis was used to interpret corrosion-inhibition mechanisms [40]. The distinctive feature of EAAP is the high efficiency at 300 ppm, high impedance resistance, and the specific concentration range where all kinds of measurements converge. Therefore, the adsorption analysis should be read in combination with the electrochemical results.

3.7 Quantum descriptors and molecular-dynamics support

Values in Table 6 provide a connection between the inhibitor performance and the electronic structure of the molecule. For caftaric acid $E_{\mathrm{HOMO}} = -5.321$ eV, $E_{\mathrm{LUMO}} = -2.902$ eV, $\Delta E = 2.419$ eV. Kaempferol-3,7-di-*O*-glucoside has $\Delta E = 2.579$ eV and the largest dipole moment equal to 12.41 Debye. For kaempferol-3-*O*-rutinoside, $\Delta N = 0.347$, while for isoquercetin $\Delta N = 0.346$. Positive values of ΔN mean the electron donation from the inhibitor molecules to the metal surface. All these values are consistent with adsorption via oxygen-rich and aromatic regions.

Table 6: Quantum descriptors.

Component	E_H	E_L	ΔE	I	A	μ	χ	η	ΔN
Caftaric acid	-5.321	-2.902	2.419	5.321	2.902	11.72	4.111	1.209	0.292
Kaempferol-3,7-di-*O*-glucoside	-5.351	-2.772	2.579	5.351	2.772	12.41	4.061	1.289	0.294
Kaempferol-3-*O*-rutinoside	-5.208	-2.658	2.550	5.208	2.658	12.18	3.933	1.275	0.347
Isoquercetin	-5.205	-2.705	2.500	5.205	2.705	11.10	3.955	1.250	0.346

From the results of DFT analysis, we can see that different molecules provide different benefits. Thus, caftaric acid provides the smallest HOMO–LUMO gap, which means the most favourable interaction of the electrons. The largest value of the dipole moment is provided by kaempferol-3,7-di-*O*-glucoside. Therefore, it supports the interaction with the electric field. The largest electron transfer fractions are characteristic of kaempferol-3-*O*-rutinoside and isoquercetin. It is a sign of donor interaction with the metal. Thus, these differences confirm the assumption that EAAP works as a molecular ensemble. Inhibitor properties do not necessarily come from one dominating compound among all descriptors but rather from several compounds combined together to create electronic reactivity, polarity and surface footprint.

The adsorption energy of molecular-dynamics inhibitors gives a more spatial picture of how the inhibitor works. Adsorption energy of caftaric acid, kaempferol-3,7-di-*O*-glucoside, kaempferol-3-*O*-rutinoside, and isoquercetin is equal to -637.1, -1107.3, -1162.9, and -810.6 kJ/mol, respectively. All values are negative, which indicates favourable adsorption on Fe(110). The absolute values are strongest for kaempferol-3-*O*-rutinoside and kaempferol-3,7-di-*O*-glucoside. These glycosylated flavonoids therefore appear to be major contributors to film stability and broad surface coverage.

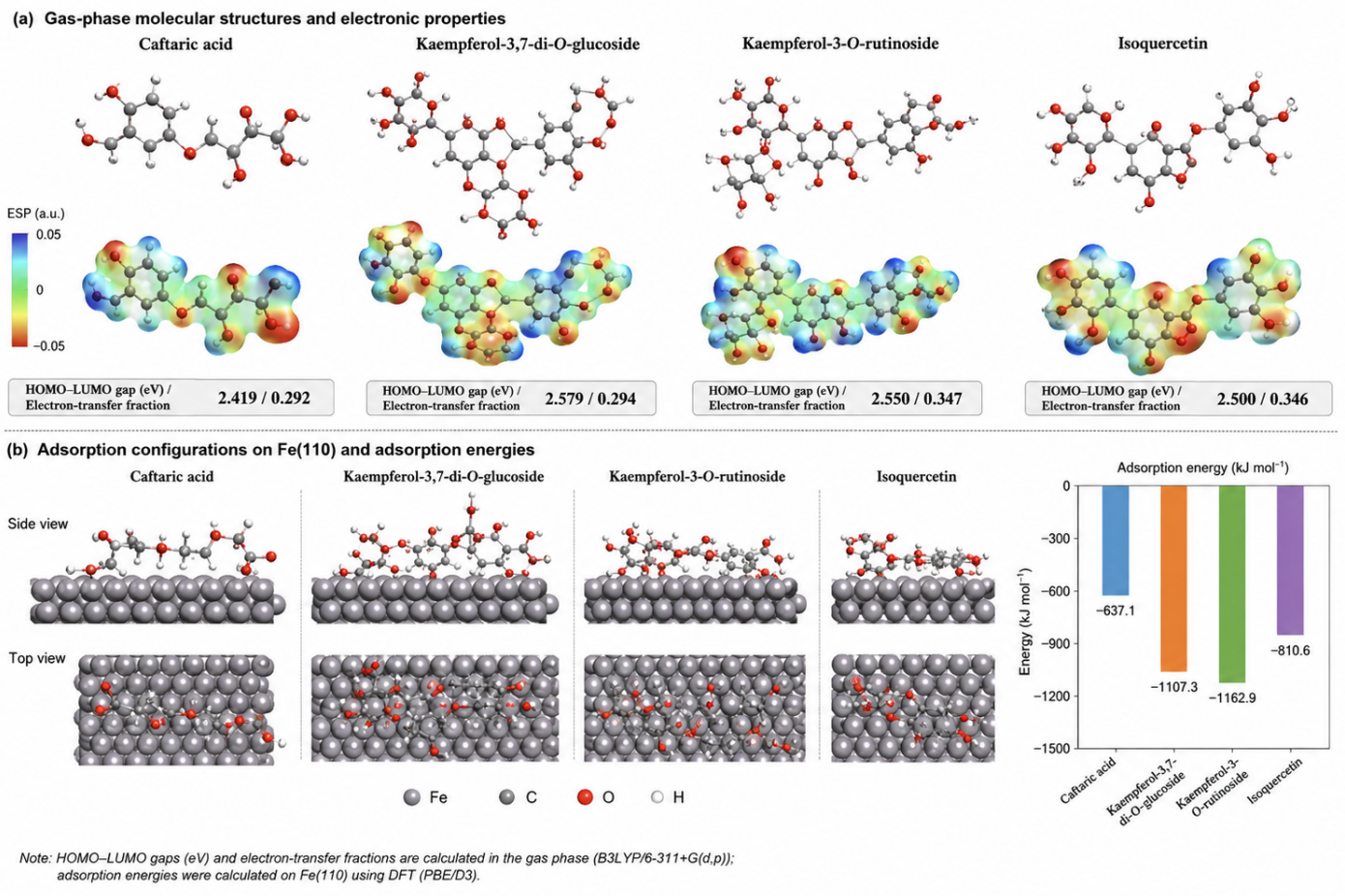

Figure 7: Molecular adsorption.

Figure 7 also provides the molecular and energy-based explanations for the experimental results: sufficient amount of protection material is required for large glycosylated molecules to occupy the surface. At lower concentration, the surface might be uneven and receive some scattered adsorption of phenolic acids and flavonoids but not necessarily continuous. At higher concentration, the strong-contact glycosides may adopt almost flat conformation and occupy larger surface area decreasing the access of acids and increase charge transfer resistance. Molecular reasoning is corroborated by the EIS data, where R_{ct} increases drastically between 50 mg/L and 100 mg/L concentrations.

It should be mentioned that the computational descriptors are not supposed to be interpreted literally as quantitative

predictors of macroscopic efficiency, since real acid solutions possess protonation equilibrium, chlorides adsorption, competition from water, surface roughness and interactions among multiple molecules. However, their use in this research is only aimed at confirmation. The presence of appropriate electronic and spatial properties for adsorption of the identified compounds by the above mentioned methods is confirmed.

3.8 Surface morphology and consolidated protection mechanism

The SEM findings provide the surface level confirmation of the electrochemical interpretation. After 4 h exposure to blank 2 M HCl solution at 298 K, the surface of the carbon-steel specimen suffers considerable damage including corrosion products formation and roughening due to active corrosion process. In turn, the sample exposed to 300 mg/L EAAP in the same acid shows significantly better preservation of the surface with lesser amounts of corrosion products. The comparison confirms that high impedance resistance and low corrosion current imply surface protection rather than curve fitting.

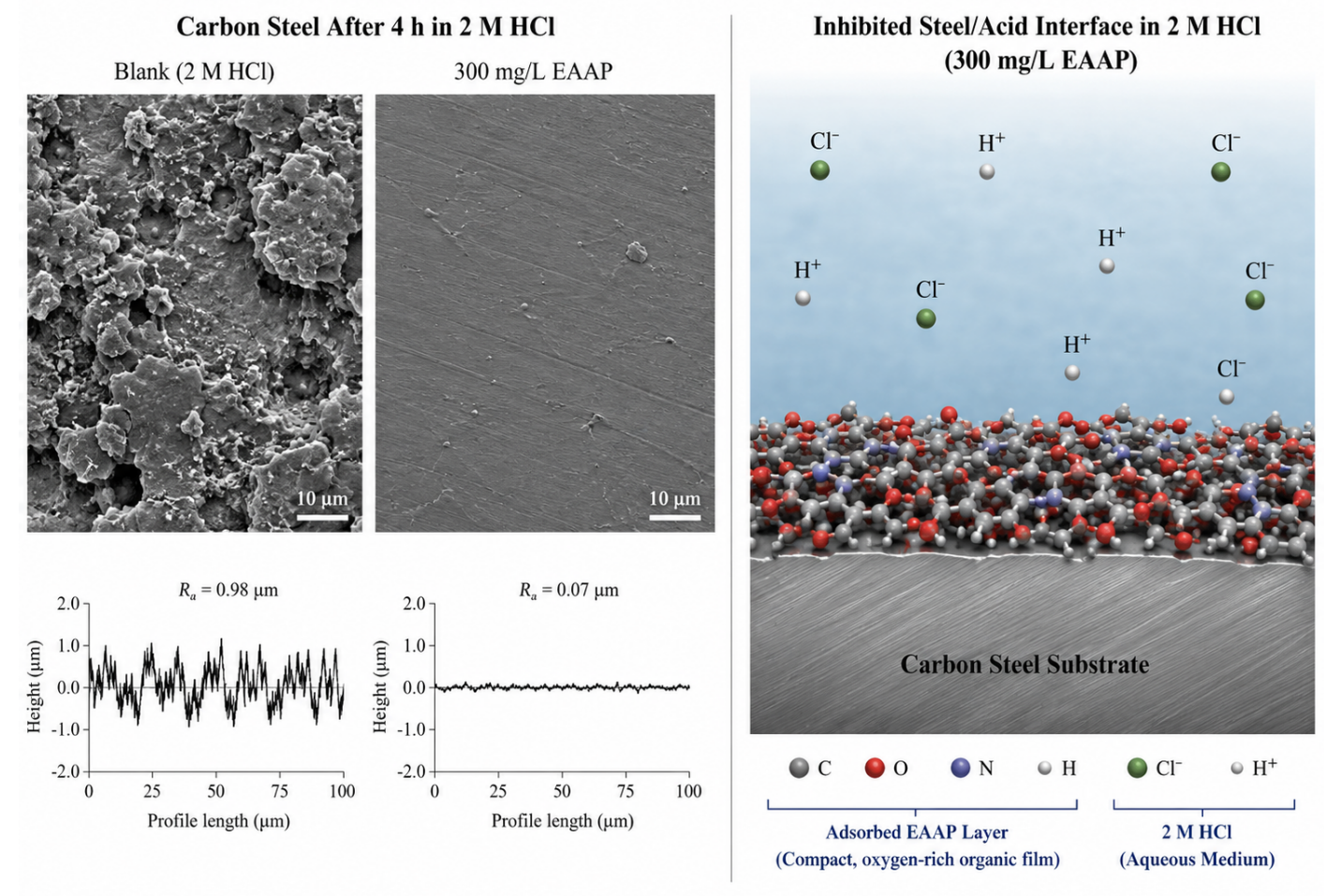

Figure 8: Surface state.

Evidence about the surface and the interface in Figure 8 can be characterized as a succession of interfacial processes. The surface images illustrate the contrast between a rough state due to acid attack and the inhibited smoother one; interfacial image illustrates the contrast at the interface of steel–solution. In the absence of the inhibitor, chloride and protons come in easy to the steel surface. Iron dissolution occurs at anodic regions, hydrogen evolution occurs at cathodic regions, and the corrosion products accumulate at a roughened surface. When the inhibitor is added, oxygen-rich molecules react with the interface of metal–solution. Protonated forms of inhibitor molecules may react with chloride-modified steel; the neutral or partially deprotonated forms may react via oxygen lone pair or aromaticity.

The mechanism is mixed physical-chemical adsorption. There are several reasons to conclude it. First of all, decrease in inhibition efficiency from 95.2% at 298 K to 89.3% at 328 K fits the picture of physical component in adsorption. Second of all, increase in activation energy and enthalpy implies that the film increases the kinetic barrier of dissolution. Positive electron-transfer fractions and negative adsorption energies indicate favorable donor interaction and adsorption. Improvement of SEM morphology implies the presence of a physical barrier on the surface. It is evident that there is no contradiction here. Evidence means that the film is formed via electrostatic and polar interactions at first, and then obtains stability via interactions with functional groups and molecule arrangement.

Role of chloride must be accounted for in the mechanism as well, not as an aggressive ion. In acidic medium, chloride may form a part of negative charge at the steel interface, which enables protonated organic molecules to attract. However, chloride is still aggressive ion because it enhances metal dissolution and destabilizes film formation. Mechanistic importance of chloride is that the same chloride-modified interface, which accelerates the corrosion, may serve as an adsorbent of inhibitor molecules when protonated phytochemical molecules are present in the interface. Studies of inhibitor adsorption in acid media reveal the role of chloride medium in inhibitor adsorption [25]. Similar studies using bamboo-leaf extract reveal that chloride medium can enable adsorption of protonated organic molecules while staying corrosive [31]. The loquat-leaf extract studies prove that corrosive chloride-rich acidic medium may enable inhibitor adsorption [39]. Dual role of chloride-rich acid solution explains why organic inhibitors work efficiently in HCl but need sufficiently high concentration to compete with water and chloride access.

Importance of surface evidence consists in that corrosion inhibition should be able to preserve morphology, not only give favorable electrochemical data. In the absence of the inhibitor in 2 M HCl, the steel surface should become rougher because dissolution does not take place uniformly at microscopic level. Differences in inclusions, grain orientation, polishing marks, and oxides residues form areas where acid attack occurs faster. Smoothness of the surface after the exposure of the inhibitor means that adsorbed molecules decrease the number of these attack points. SEM is thus the physical proof of the charge transfer and mass loss results.

Preservation of morphology has practical importance for the cleaning operations. Roughened steel surface may hold deposits easier, cause flow disturbance, and create new attack points in the future. Protection of corrosion during cleaning protects not only the thickness but also the future fouling behavior of the equipment. The EAAP protection is important in such wider sense of maintenance because the inhibited surface is not only less dissolved; it is also less damaged as an engineering surface.

The consolidated film is likely to be heterogeneous. Phenolic acids may attach or associate close to high-energy regions, while kaempferol glycosides and flavonoids may orient themselves on Fe(110)-like surfaces. Isoquercetin and other flavonoids may provide extra oxygen-rich anchoring sites and aromatic contacts. Hydrogen bonds between hydroxyl and glycosidic groups can help the cohesion of the layer. Such layer is not a perfect monolayer, but it is cohesive enough to prevent charge transfer. Difference between cohesive layer and monolayer is significant because the idealized language of monolayer gives the impression of greater certainty about plant-extract mechanisms than the actual data allow. The evidence suggests compact and mixed adsorbed layer of phytochemical molecules rather than the film of the uniform molecule.

3.9 Comparison with other botanical inhibitors and practical relevance

The comparative data in Table 7 compare the effectiveness of EAAP with other botanical inhibitors in steel in 2 M HCl. Aizoon canariense inhibitor achieved 82.6% at 250 ppm, olive leaf extract achieved 91.0% at 900 ppm, *Conyza bonariensis* achieved 93.3% at 100 ppm, *Rosmarinus officinalis* achieved 89.18% at 200 ppm, eggplant peel achieved 84.0% at 1000 ppm, *Baphia nitida* leaves achieved 93.0% at 100 ppm, and *Tectona grandis* leaf extract achieved 71.7% at 1000 ppm. EAAP achieves 97.4% at 300 ppm. The comparison shows that EAAP is not only effective in an absolute sense but competitive within the specific acid strength.

Table 7: Botanical-inhibitor comparison.

Extract	Optimum concentration	Medium	Maximum efficiency (%)
Aizoon canariense [41]	250 ppm	2 M HCl	82.6
Olive leaf extract [42]	900 ppm	2 M HCl	91.0
Conyza bonariensis [43]	100 ppm	2 M HCl	93.3
Rosmarinus officinalis [44]	200 ppm	2 M HCl	89.18
Eggplant peel [45]	1000 ppm	2 M HCl	84.0
Baphia nitida leaves [46]	100 ppm	2 M HCl	93.0
Tectona grandis leaf [47]	1000 ppm	2 M HCl	71.7
Equisetum arvense aerial part [48]	300 ppm	2 M HCl	97.4

The comparison in Table 7 is to be understood as an illustration of the data, which cannot be considered ranking in isolation from the experiment. Differences in steel grade, surface preparation, exposure time, hydrodynamics, temperature, extract concentration, and efficiency calculation may affect performance. However, the data can be helpful as it shows that all tested systems involve steel and 2 M HCl solution. EAAP demonstrates excellent performance at moderate concentration, and the evidence package is unusually comprehensive as it involves HPLC, FTIR, gravimetry, polarization, EIS, thermal analysis, Langmuir adsorption, DFT, MD, and SEM. Most botanical-inhibitor studies report only a subset of this chain.

The practical comparison allows seeing the importance of the concentration unit. Some extracts demonstrate acceptable efficiencies at 900 ppm or 1000 ppm, which is tolerable for laboratory screening but much less attractive for plant-scale

circulation where organic load, foaming, spent-acid processing, and reproducibility issues arise. EAAP achieves 97.4% polarization efficiency at 300 ppm and 95% of gravimetric inhibition at the same concentration. Moderate dosage combined with multiple measurements makes it one of the most convincing green inhibitors in strong HCl solution.

In order to make an adequate comparison, it is necessary to remember that plant extracts are chemically heterogeneous substances. Variations in solvent ratio, extraction temperature, botanical source, drying, and storage period influence the relative proportion of phenolic acids and flavonoid glycosides in the extract. HPLC identity list allows for initial chemical profiling, however, further development will require quantitative standardization by chromatography. For instance, certain minimal content of kaempferol glycosides or oxygenated phenolic compounds can be used as quality control criteria. Without standardization, 300 ppm of one extract batch will not be chemically equal to the same nominal concentration of another batch.

Practical significance of EAAP can be seen in the context of acid cleaning. In desalination and water treatment equipment, an inhibitor should perform while scale removal takes place and while the acid is aggressive. The inhibitor is not supposed to neutralize the acid, because it would reduce the efficiency of cleaning. EAAP, however, functions in the interface, where adsorption protects the metal while allowing the bulk acid to remain available for scale removal. High efficiency at 300 ppm and retention of efficiency at 328 K makes the extract promising for studying under conditions more relevant to plant operation, such as long exposure, cyclic cleaning, brine contamination, dissolved scale products, and dynamic geometries with complex turbulence.

Final practical aspect relates to further test design based on the obtained evidence. The optimal continuation of the research is not just repetition of the four-hour exposure test at different concentrations. Data show major concentration transition point and high efficiency at 300 ppm. Further research should address cycling, spent-acid chemistry, steel grades with different microstructures, and interaction of EAAP with the dissolved scale products, such as calcium, magnesium, iron, and silica ions. These factors can influence adsorption process, making it more or less efficient. If EAAP retains its efficiency under these conditions, the case of this phytochemical as a cleaning service inhibitor becomes much stronger.

Alongside with further research, the standardization of the inhibitor is required. Reproducible inhibitor cannot be identified solely by the plant name, because botanical material is variable. The optimal specification will involve extract concentration, chromatographic identification markers, total phenolic compound content, moisture, and solvent composition. Caftaric acid, kaempferol glycosides, isoquercetin, astragalin, and cichoric acid peaks in the HPLC can be used as such identification markers. Coupling the chemical profiling with corrosion testing will put the development of EAAP inhibitor in line with contemporary green inhibitor studies, where chemical and electrochemical properties are evaluated jointly [11, 13].

Evidentiary base also shows several limitations which have to be addressed before moving to industrial use. The extract composition depends on plant origin, harvesting season, drying and storage methods, particle size, and solvent ratio. HPLC analysis reveals twelve components, however, the quantitative peak area and batch-to-batch variability are required for standardization. Long-term stability, compatibility with other additives, foaming tendency, spent acid organic load, and interaction with spent-acid treatment process have to be investigated. These limitations do not weaken the presented inhibition in 2 M HCl, they show the further requirements for converting the promising inhibitor into reproducible chemical additive.

3.10 Integrated interpretation of the corrosion-inhibition state

The most reliable conclusion comes from converging independent measurements. HPLC and FTIR analysis shows that the extract has oxygenated components capable of adsorption. Mass loss analysis demonstrates the significant reduction of the dissolution. Polarization demonstrates more than an order of magnitude decrease in corrosion current density and mixed inhibition type. EIS shows nearly thirtyfold increase in charge transfer resistance and sharp reduction of the constant phase element parameter. Temperature data show that the film is still protective after heating, however, has some physical adsorption components. Adsorption analysis connects efficiency with surface coverage. DFT and MD show favorable molecular properties and strong adsorption energies, particularly kaempferol glycosides. SEM demonstrates preservation of the inhibited surface.

Concentration dependence gives specificity to the interpretation. At 25 mg/L, EAAP provides the limited protection because of low adsorbate concentration. At 50 mg/L, the inhibitor shows more pronounced efficiency but leaves considerable exposed area. At 100 mg/L, the interface changes its character: mass-loss efficiency goes to 91.7%, polarization efficiency goes to 93.2%, and impedance efficiency goes to 95.7%. This is the first concentration where all three main measures of efficiency show strong protection. At 200 mg/L and 300 mg/L concentrations, the performance is improved but marginally, which means that surface is already mostly controlled.

The combined evidence shows that high efficiency is not just the percent value. The concentration dependence, oxygenated adsorption chemistry, electrochemical suppression, thermal behavior, computational adsorption analysis, and

surface preservation all point to the same state of the interface. EAAP is chemically plausible, electrochemically active, thermally interpretable, computation-supported, and morphologically proved. Different techniques address different aspects of the corrosion process and give consistent answers.

The strongest evidence is cumulative. Alone, the chemical evidence would show that EAAP has chemically plausible adsorption groups but would not prove protection. Alone, the gravimetric evidence would show reduced mass loss but would not prove whether the anodic and cathodic processes are affected. Alone, the polarization evidence would show kinetic suppression but would not prove film compactness. Alone, the impedance evidence would show the resistive nature of the interface but would not reveal molecules forming it. Temperature, adsorption, DFT, MD, and SEM fill gaps in this evidentiary chain. Agreement of these independent measures makes the claim about inhibition strong as it shows the same transition in different aspects of the process.

Also, this cumulative interpretation explains the plateau above 100 mg/L. After reaching high surface coverage, increasing the concentration of the extract cannot provide unlimited reduction of corrosion, since it can proceed in defect areas, transient pores, high energy sites, and places where flow and gas evolution disturb the organic layer. The lack of increase in efficiency between 200 mg/L and 300 mg/L is not the flaw but the evidence that the limiting interfacial state is achieved. This feature is beneficial for practical use, because it reveals the concentration region where additional dosage provides decreasing efficiency gains and optimization should take into account the cost, environmental impact, and compatibility rather than efficiency alone.

The scientific value of this interpretation is conversion of the set of corrosion-related measurements into consistent answer about the state where and why the interface becomes protective. The transition point at 100 mg/L is not random: it is the first point where the practical mass loss, instantaneous corrosion current, and interfacial resistance are all high. The maximal point at 300 mg/L proves that the protective state can be strengthened without changing its nature. The difference between the transition point and maximal point provides more accurate answer than single efficiency value.

The order of evidence is crucial as it ensures that each measurement is interpreted within the same framework of the interfacial question. HPLC and FTIR show why adsorption is possible. Gravimetry, polarization, and impedance show when protection starts. Temperature response, adsorption analysis, DFT, MD, and SEM explain why the protection is maintained and how the molecules interact with the surface. Such interpretation structure prevents the discussion from turning into the list of techniques and ensures contribution of each measurement into answering the scientific question.

Evidentiary base also allows providing balanced interpretation regarding environment-related advantages of the substance. EAAP is promising because of high inhibition at moderate concentration, however, its green characteristics should be proved with corrosion performance and process compatibility. Botanical origin, oxygen-rich chemistry, and high efficiency are the positive features, however, reproducible extraction process, spent-acid treatment, and compatibility with cleaning procedures are still required. The data allow considering the extract as a credible candidate for acid cleaning protection, defining the tests required for going beyond laboratory and getting the controlled operational usage.

Therefore, the research question is answered directly. EAAP extract provides stabilization of carbon steel in 2 M HCl by forming the adsorbed phytochemical layer, which progressively converts the interface from chloride-accessible active dissolution to charge transfer restricted protective state. The critical transition is achieved around 100 mg/L while 300 mg/L is the point of maximal measured performance. The mechanism of this process cannot be attributed to single molecule or electrochemical pathway. It comes from the cooperative adsorption of phenolic acids and flavonoid glycosides with broad-surface interactions of kaempferol derivatives, oxygen-rich interactions, and reduction of water and chloride accessibility at the metal surface.

4. Conclusion

The central research question was whether *Equisetum arvense* aerial-part extract can provide coherent corrosion inhibition state on carbon steel in 2 M HCl and which evidence can best show the transition to the state of strong protection. The answer is positive. EAAP creates mixed adsorbed phytochemical layer, which suppresses acid corrosion by providing the interface transformation from the chloride-accessible active dissolution to charge transfer restriction with adsorption-active chemistry. The best evidence is the simultaneous transition from 50 mg/L to 100 mg/L where mass-loss efficiency increases from 47.8% to 91.7%, polarization efficiency increases from 77.3% to 93.2%, and impedance efficiency increases from 81.4% to 95.7%. This evidence shows that the interface transitions from partial site occupation to the protective state.

At 300 mg/L, EAAP provides the maximal inhibition. Corrosion rate decreases from 12.23 ± 0.33 µg/(cm^2 h) to 0.58 ± 0.02 µg/(cm^2 h); j_{corr} decreases from 511.5 µA/cm^2 to 13.2 µA/cm^2; R_{ct} increases from 35.7 Ω cm^2 to 1054.9 Ω cm^2; and CPE decreases from 725.4 µF/cm^2 to 89.9 µF/cm^2. These values show that the inhibitor decreases real metal loss, reduces the electrochemical kinetics, and transforms the interface into resistive and less capacitive state.

The chemical reason behind this performance is the presence of twelve oxygenated compounds, including caftaric acid, kaempferol glycosides, quercetin-3,7-di-O-glucoside, isoquercetin, astragalin, and cichoric acid. FTIR analysis reveals hydroxyl, carbonyl, aliphatic, and deformation vibrations. DFT analysis shows positive electron transfer fraction values, while molecular dynamics adsorption energies show the favorable adsorption onto Fe(110), especially kaempferol-3-O-rutinoside and kaempferol-3,7-di-O-glucoside. Temperature behavior and the Langmuir equation show the importance of physical adsorption, however, SEM preservation and computational analysis show the sufficient stability to maintain the protective film in the heated acid solution.

Thus, EAAP is the credible green inhibitor candidate for protection of carbon steel during hydrochloric acid cleaning due to the multicomponent phytochemical layer adsorption blocking anodic and cathodic sites of the metal. The remaining research requirement is not the proof of the inhibiting effect, which is already provided, but the standardization of the extract composition, verification in the acid cleaning cycles, compatibility with industrial cleaning additives, and spent-acid treatment needs.

Conflict of Interest

The author declares no conflict of interest.

References

[1] Malik, A. U., Ahmad, S., Andijani, I., Asrar, N., Al-Mobayed, A. S., & Al-Jardan, A. M. (1997). Acid cleaning of some Desal units at Al-Jubail plant (pp. 1575-1618). Technical Report No. TR3804/APP95007.

[2] Amjad, Z. (1996). Scale Inhibition in Desalination Applications: An Overview. The NACE International Annual Conference and Exposition. Corrosion, Paper No, 230.

[3] Jones, E., Qadir, M., Van Vliet, M. T., Smakhtin, V., & Kang, S. M. (2019). The state of desalination and brine production: A global outlook. Science of the total environment, 657, 1343-1356.

[4] Ghaffour, N., Missimer, T. M., & Amy, G. L. (2013). Technical review and evaluation of the economics of water desalination: Current and future challenges for better water supply sustainability. Desalination, 309, 197-207.

[5] Sastri, V. S. (2010). Corrosion inhibitors: other important applications.

[6] Frenier, W. W. (1998, March). Strategies for formulating low hazard corrosion inhibitors for use in chemical cleaning solvents, NACE 98338. In NACE Int. Conf.(San Diego, Carlifornia, USA) (Vol. 27, p. 22).

[7] Obot, I. B., Onyeachu, I. B., Wazzan, N., & Al-Amri, A. H. (2019). Theoretical and experimental investigation of two alkyl carboxylates as corrosion inhibitors for steel in acidic medium. Journal of Molecular Liquids, 279, 190-207.

[8] Bentiss, F., Traisnel, M., & Lagrenee, M. (2000). The substituted 1, 3, 4-oxadiazoles: a new class of corrosion inhibitors of mild steel in acidic media. Corrosion science, 42(1), 127-146.

[9] Quraishi, M. A., & Jamal, D. (2003). Dianils as new and effective corrosion inhibitors for mild steel in acidic solutions. Materials chemistry and physics, 78(3), 608-613.

[10] Kokalj, A. (2010). Is the analysis of molecular electronic structure of corrosion inhibitors sufficient to predict the trend of their inhibition performance. Electrochimica Acta, 56(2), 745-755.

[11] Sheydaei, M. (2024). The use of plant extracts as green corrosion inhibitors: A review. Surfaces, 7(2), 380-403.

[12] de Souza Morais, W. R., da Silva, J. S., Queiroz, N. M. P., de Paiva e Silva Zanta, C. L., Ribeiro, A. S., & Tonholo, J. (2023). Green corrosion inhibitors based on plant extracts for metals and alloys in corrosive environment: a technological and scientific prospection. Applied Sciences, 13(13), 7482.

[13] Thacker, H., & Ram, V. (2025). Green corrosion inhibitors derived from plant extracts and drugs for mild steel in acid media: A review. Results in Surfaces and Interfaces, 18, 100364.

[14] Alimohammadi, M., Ghaderi, M., Ramazani SA, A., & Mahdavian, M. (2023). Falcaria vulgaris leaves extract as an eco-friendly corrosion inhibitor for mild steel in hydrochloric acid media. Scientific Reports, 13(1), 3737.

[15] Pourmohseni, M., Rashidi, A., & Karimkhani, M. (2024). Preparation of corrosion inhibitor from natural plant for mild stil immersed in an acidic environmental: experimental and theoretical study. Scientific Reports, 14(1), 7937.

[16] Naghizade, R., Sajadi, G. S., Mashizi, A. K., Golshani, Z., Amiri, M., & Hosseini, S. M. A. (2024). Investigation of mild steel corrosion inhibition in acidic media by Viola extract based on bulk and nanometer size. Scientific Reports, 14(1), 15455.

[17] Rizi, A., Sedik, A., Acidi, A., Rachedi, K. O., Ferkous, H., Berredjem, M., ... & Benguerba, Y. (2023). Sustainable and green corrosion inhibition of mild steel: insights from electrochemical and computational approaches. ACS omega, 8(49), 47224-47238.

[18] Carmona-Hernandez, A., Barreda-Serrano, M. C., Saldarriaga-Noreña, H. A., López-Sesenes, R., González-Rodríguez, J. G., Mejía-Sánchez, E., ... & Galván-Martínez, R. (2024). Insight into the corrosion inhibition performance of Pistia stratiotes leaf extract as a novel eco-friendly corrosion inhibitor for mild steel in 1 M HCl solution. Molecules, 29(22), 5243.

[19] Boeing, T., Tafarelo Moreno, K. G., Gasparotto Junior, A., Mota da Silva, L., & De Souza, P. (2021). Phytochemistry and pharmacology of the genus Equisetum (Equisetaceae): A narrative review of the species with therapeutic potential for kidney diseases. Evidence-Based Complementary and Alternative Medicine, 2021(1), 6658434.

[20] Ramírez-Peralta, G. I., León-Silva, U., Nicho Díaz, M. E., & Valladares-Cisneros, M. G. (2018). Effect of Equisetum arvense extract as corrosion inhibitor of A36 steel in sulfuric acid solution. Materials and Corrosion, 69(11), 1631-1637.

[21] Deyab, M. A., Mohsen, Q., & Guo, L. (2022). Theoretical, chemical, and electrochemical studies of Equisetum arvense extract as an impactful inhibitor of steel corrosion in 2 M HCl electrolyte. Scientific Reports, 12(1), 2255.

[22] LS, L. G. (2011). Standard Practice for Preparing, Cleaning, and Evaluation Corrosion Test Specimens.

[23] Mansfeld, F., Kendig, M. W., & Tsai, S. (1982). Recording and analysis of AC impedance data for corrosion studies II. Experimental approach and results. Corrosion, 38(11), 570-580.

[24] Langmuir, I. (1918). The adsorption of gases on plane surfaces of glass, mica and platinum. Journal of the American Chemical society, 40(9), 1361-1403.

[25] Solmaz, R. (2014). Investigation of adsorption and corrosion inhibition of mild steel in hydrochloric acid solution by 5-(4-Dimethylaminobenzylidene) rhodanine. Corrosion Science, 79, 169-176.

[26] Guo, L., Kaya, S., Obot, I. B., Zheng, X., & Qiang, Y. (2017). Toward understanding the anticorrosive mechanism of some thiourea derivatives for carbon steel corrosion: A combined DFT and molecular dynamics investigation. Journal of colloid and interface science, 506, 478-485.

[27] Guo, L., Tan, B., Li, W., Li, Q., Zheng, X., & Obot, I. B. (2021). Banana leaves water extracts as inhibitor for X70 steel corrosion in HCl medium. Journal of Molecular Liquids, 327, 114828.

[28] Alibakhshi, E., Ramezanzadeh, M., Haddadi, S. A., Bahlakeh, G., Ramezanzadeh, B., & Mahdavian, M. (2019). Persian Liquorice extract as a highly efficient sustainable corrosion inhibitor for mild steel in sodium chloride solution. Journal of cleaner production, 210, 660-672.
[29] Dehghani, A., Bahlakeh, G., & Ramezanzadeh, B. (2019). A detailed electrochemical/theoretical exploration of the aqueous Chinese gooseberry fruit shell extract as a green and cheap corrosion inhibitor for mild steel in acidic solution. Journal of Molecular Liquids, 282, 366-384.
[30] Umoren, S. A., Eduok, U. M., Solomon, M. M., & Udoh, A. P. (2016). Corrosion inhibition by leaves and stem extracts of Sida acuta for mild steel in 1 M H2SO4 solutions investigated by chemical and spectroscopic techniques. Arabian journal of chemistry, 9, S209-S224.
[31] Li, X., Deng, S., Xie, X., & Fu, H. (2014). Inhibition effect of bamboo leaves' extract on steel and zinc in citric acid solution. Corrosion Science, 87, 15-26.
[32] Mourya, P., Banerjee, S., & Singh, M. M. (2014). Corrosion inhibition of mild steel in acidic solution by Tagetes erecta (Marigold flower) extract as a green inhibitor. Corrosion Science, 85, 352-363.
[33] Deng, S., & Li, X. (2012). Inhibition by Ginkgo leaves extract of the corrosion of steel in HCl and H2SO4 solutions. Corrosion Science, 55, 407-415.
[34] Al-Otaibi, M. S., Al-Mayouf, A. M., Khan, M., Mousa, A. A., Al-Mazroa, S. A., & Alkhathlan, H. Z. (2014). Corrosion inhibitory action of some plant extracts on the corrosion of mild steel in acidic media. Arabian Journal of Chemistry, 7(3), 340-346.
[35] Nematian, B., Ramazani, S. A., Mahdavian, M., Bahlakeh, G., & Haddadi, S. A. (2020). Adsorption of eco-friendly carthamus tinctorius on steel surface in saline solution: A combination of electrochemical and theoretical studies. Colloids and Surfaces A: Physicochemical and Engineering Aspects, 601, 125042.
[36] Yadav, D. K., Quraishi, M. A., & Maiti, B. (2012). Inhibition effect of some benzylidenes on mild steel in 1 M HCl: an experimental and theoretical correlation. Corrosion science, 55, 254-266.
[37] El-Etre, A. Y. (2007). Inhibition of acid corrosion of carbon steel using aqueous extract of olive leaves. Journal of colloid and interface science, 314(2), 578-583.
[38] Njoku, V. O., Oguzie, E. E., Obi, C., & Ayuk, A. A. (2014). Baphia nitida leaves extract as a green corrosion inhibitor for the corrosion of mild steel in acidic media. Advances in Chemistry, 2014(1), 808456.
[39] Zheng, X., Gong, M., Li, Q., & Guo, L. (2018). Corrosion inhibition of mild steel in sulfuric acid solution by loquat (Eriobotrya japonica Lindl.) leaves extract. Scientific reports, 8(1), 9140.
[40] Kadapparambil, S., Yadav, K., Ramachandran, M., & Victoria Selvam, N. (2017). Electrochemical investigation of the corrosion inhibition mechanism of Tectona grandis leaf extract for SS304 stainless steel in hydrochloric acid. Corrosion Reviews, 35(2), 111-121.
[41] Fouda, A. E. S., Motaal, S. M. A., Ahmed, A. S., Sallam, H. B., Ezzat, A., & El-Hossiany, A. (2021). Corrosion protection of carbon steel in 2M HCl using aizoon canariense extract. Biointerface Res. Appl. Chem, 12(1), 230-243.
[42] El-Etre, A. Y. (2007). Inhibition of acid corrosion of carbon steel using aqueous extract of olive leaves. Journal of colloid and interface science, 314(2), 578-583.
[43] Al-Sallami, K. J., Shalabi, K., & Fouda, A. S. (2021). Impact of Conyza bonariensis extract on the corrosion protection of carbon steel in 2 M HCl solution. International Journal of Electrochemical Science, 16(9), 210929.
[44] Belakhdar, A., Ferkous, H., Djellali, S., Sahraoui, R., Lahbib, H., & Ben Amor, Y. (2020). Corrosion Inhibition Performance of Rosmarinus officinalis Methanolic Ex-tract on Carbon Steel XC48 in Acidic Medium (2M HCl). Materials & biomaterials science, 3(2), 46-53.
[45] Ibrahim, T., & Habbab, M. (2011). Corrosion inhibition of mild steel in 2M HCl using aqueous extract of eggplant peel. International Journal of Electrochemical Science, 6(11), 5357-5371.
[46] Njoku, V. O., Oguzie, E. E., Obi, C., & Ayuk, A. A. (2014). Baphia nitida leaves extract as a green corrosion inhibitor for the corrosion of mild steel in acidic media. Advances in Chemistry, 2014(1), 808456.
[47] Kadapparambil, S., Yadav, K., Ramachandran, M., & Victoria Selvam, N. (2017). Electrochemical investigation of the corrosion inhibition mechanism of Tectona grandis leaf extract for SS304 stainless steel in hydrochloric acid. Corrosion Reviews, 35(2), 111-121.
[48] Deyab, M. A., Mohsen, Q., & Guo, L. (2022). Theoretical, chemical, and electrochemical studies of Equisetum arvense extract as an impactful inhibitor of steel corrosion in 2 M HCl electrolyte. Scientific Reports, 12(1), 2255.